

Glass transition memorized by the enthalpy-entropy compensation in the shear thinning of supercooled metallic liquids

Meng Zhang^{1,2,3}  and Lin Liu³

¹ Institute of Advanced Wear and Corrosion Resistant and Functional Materials, Jinan University, Guangzhou 510632, People's Republic of China

² State Key Laboratory of Nonlinear Mechanics, Institute of Mechanics, Chinese Academy of Sciences, Beijing 100190, People's Republic of China

³ School of Materials Science and Engineering, Huazhong University of Science and Technology, Wuhan 430074, People's Republic of China

E-mail: m.zhangjwrm@jnu.edu.cn

Received 29 March 2018, revised 27 April 2018

Accepted for publication 3 May 2018


Published 21 May 2018



Abstract

To unravel the true nature of glass transition, broader insights into glass forming have been gained by examining the stress-driven glassy systems, where strong shear thinning, i.e. a reduced viscosity under increasing shear rate, is encountered. It is argued that arbitrarily small stress-driven shear rates would 'melt' the glass and erase any memory of its thermal history. In this work, we report a glass transition memorized by the enthalpy-entropy compensation in strongly shear-thinned supercooled metallic liquids, which coincides with the thermal glass transition in both the transition temperature and the activation Gibbs free energy. Our findings provide distinctive insights into both glass forming and shear thinning, and enrich current knowledge on the ubiquitous enthalpy-entropy compensation empirical law in condensed matter physics.

Keywords: metallic glasses, glass transition, shear thinning, enthalpy-entropy compensation

 Supplementary material for this article is available [online](#)

(Some figures may appear in colour only in the online journal)

1. Introduction

The effort to understand the mysterious glass formation phenomenon [1] is frustratingly hindered by the procedure known as aging [2, 3], in which glasses spontaneously evolve extremely slowly towards the equilibrium state due to their out-of-equilibrium nature. To circumvent this situation, stress-driven glassy systems which exhibit strong shear thinning (i.e. a reduced viscosity under increasing shear rate) have been intensively examined [4–10]. The stress-driven flow characterized by a shear rate will create a non-equilibrium while steady state, in which the aging of glassy systems is interrupted and the time translation invariance is recovered [5, 11]. This steady state can thus be examined to provide broader insights into glassy physics, by easily adopting the shear rate

rather than the natural aging time of glasses as the control parameter. As evidenced by the effective temperature [5, 12] and the most probable atomic displacement [13], a scaling relationship between stress and temperature as they affect the glassy systems has been confirmed as both of them could reduce the viscosity and 'melt' a glass into a liquid [14–16]. Hence, it is argued that an arbitrarily small shear rate exerted on a glass is able to melt the glass into a liquid and thus erase any memory of its thermal history in glassy state [5, 6, 11].

However, in this work, by virtue of the thermodynamic enthalpy-entropy compensation law (or known as the Meyer–Neldel (MN) rule) [17] which reads $\Delta H = T_{MN}\Delta S$ and prevails in diverse processes [18–21] in condensed matter physics, where ΔH is the activation enthalpy; ΔS is the activation entropy; and T_{MN} is the iso-kinetic compensation temperature,

we found a glass transition memorized in strongly shear-thinned supercooled liquids. The memorized glass transition coincides with the thermal glass transition in both the glass transition temperature and the activation Gibbs free energy ΔG , suggesting a kinetic nature of the glass forming process and an intrinsic correlation between thermal glass forming and stress-driven shear thinning. The origin of the enthalpy-entropy compensation in supercooled liquids is attributed to the multiple-excitation effect [22], i.e. the facilitation effect and the correlation effect in the activation of shear transformation zones (STZs) [23–25].

2. Methods and experimental

Due to the structural similarity to the dense random packing of spheres [26], supercooled metallic liquids (SMLs) represent an ideal research subject for the current study. The enthalpy-entropy compensation law in the shear thinning of $Zr_{58.5}Cu_{15.6}Al_{10.3}Ni_{12.8}Nb_{2.8}$ (Vit106a) and $Zr_{41.2}Ti_{13.8}Cu_{12.5}Ni_{10}Be_{22.5}$ (Vit1) SMLs are verified by the linear relationship between the activation entropy ΔS and the activation enthalpy ΔH in the flow of SMLs.

To determine the activation entropy ΔS and the activation enthalpy ΔH , the transition state theory (TST) based flow model of SMLs [27, 28] is adopted, where STZ is envisioned as the elementary excitation event of the thermally assisted activation process in the flow of SMLs. In the STZ model, the flow equation of SMLs reads [27]: $\dot{\epsilon} = \dot{\epsilon}_0 \exp(-\Delta G(T, \sigma)/k_B T)$, where $\Delta G(T, \sigma) = \Delta H - T\Delta S = \Delta Q - \sigma V - T\Delta S$ is the activation Gibbs free energy for the flow of SML. $\dot{\epsilon}$ is the strain rate. $\dot{\epsilon}_0$ is a pre-factor that defines the upper limit of the flow rate of SMLs. σ is the steady state flow stress. T is temperature. k_B is Boltzmann's constant. ΔQ is the activation energy for the flow of SML. V is the activation volume for the flow of SML. Since the temperature dependence of ΔS and ΔH is weak [19], ΔS and ΔH are considered as constants at given flow stress. Therefore, based on the linear relationship: $\Delta G = \Delta H - T\Delta S$, the crucial step to derive ΔS and ΔH is to determine the dependence of ΔG on temperature T . Whereby, ΔS can be determined from the slope of the linear relationship (ΔG versus T), and ΔH can be determined from the intercept of the linear relationship (ΔG versus T) with the coordinate axis. It is noted that $\Delta G(T, \sigma)$ is a function of both temperature T and flow stress σ . Under different flow stresses σ , different linear relationships (ΔG versus T) can be derived. Therefore, the relationship between the activation entropy ΔS and the activation enthalpy ΔH at different flow stresses in the flow of SMLs can be examined.

As a function of temperature T and flow stress σ , $\Delta G(T, \sigma)$ can be written as $\Delta G(T, \sigma) = k_B T \ln(\dot{\epsilon}_0/\dot{\epsilon})$ based on the above flow equation. In Argon's seminal work [29], $\dot{\epsilon}_0$ reads $\dot{\epsilon}_0 = \alpha v_0 \epsilon_{\text{unit}}$, where α is a geometric factor depending on the shape of STZ; v_0 is the attempt frequency; and ϵ_{unit} is the unit strain carried by an STZ. Specifically, α is in the range 0.1–0.2. v_0 is of a order of magnitude of 10^{12} Hz. ϵ_{unit} is also of a order of 0.1. Therefore, to determine the temperature and flow stress together dependent $\Delta G(T, \sigma)$, the

steady state flow stress σ of the 2 SMLs are measured in a wide range of strain rate $\dot{\epsilon}$ from 10^{-3} s^{-1} to 10^0 s^{-1} and at different temperatures T (see supplemental materials SI (stacks.iop.org/JPhysCM/30/245401/mmedia) for more details on the experimental tests, figures S1 and S2), as shown in figures 1(a) and (b). Based on the combination $(T, \sigma(\dot{\epsilon}))$ of the experimental temperature T and the measured steady state flow stress at different strain rates $\sigma(\dot{\epsilon})$, the dependence of ΔG on temperature and flow stress of the 2 SMLs can be obtained by substituting the corresponding strain rate into the equation: $\Delta G(T, \sigma) = k_B T \ln(\dot{\epsilon}_0/\dot{\epsilon})$. Consequently, the activation entropy ΔS and activation enthalpy ΔH in the flow of SMLs under different flow stresses can be readily derived by fitting the dependence of ΔG on temperature with the linear relationship: $\Delta G = \Delta H - T\Delta S$, as will be shown in the following sections.

3. Results and discussion

3.1. Activation enthalpy and activation entropy

Figures 1(c) and (d) show the strain rate sensitivity index $m^* = \partial \ln \sigma / \partial \ln \dot{\epsilon}$ derived from the steady state flow stress σ at different strain rates $\dot{\epsilon}$ of the 2 SMLs (see supplemental materials SI, figure S2). A clear decrease of m^* from ~ 0.7 to nearly 0 is displayed, indicating a strong shear thinning phenomenon in the steady state flow of the 2 SMLs at different temperatures. Figures 2(a) and (b) plot the ΔG derived from $\Delta G(T, \sigma) = k_B T \ln(\dot{\epsilon}/\dot{\epsilon}_0)$ against the steady state flow stress σ of Vit106a and Vit1 SMLs at different temperatures T , respectively. It can be seen that ΔG decreases monotonously with both increasing σ and increasing T . This phenomenon reflects the stress-temperature scaling in the activation dynamics of STZs in the steady state flow of SMLs [14, 30]. This is because that the effect of σ similar to T could also reduce the activation energy barrier on the local potential energy landscape, thereby 'melting' a glass into a liquid. With the group of ΔG versus σ relations at different temperature T presented in figures 2(a) and (b), the ΔG versus T relations under different flow stresses can be conveniently interpolated.

Figures 3(a) and (b) show the ΔG versus T relations interpolated from figure 2 to the first approximation for Vit106a and Vit1 SMLs, respectively. It can be seen that, consistent with figure 2, ΔG decreases monotonously with increasing T at constant flow stress and decreases with increasing σ at constant temperature. Linear fits of the relationship between ΔG and T can be obtained for the 2 SMLs, except for small deviations of ΔG at 633 K for Vit1 SML, which will be discussed later. The linear relationship between ΔG and T confirms that ΔS and ΔH are approximately independent of temperature and could be treated as constants at given flow stress. Based on the equation: $\Delta G = \Delta H - T\Delta S$, ΔS is determined from the slope of the fit of ΔG versus T relations; ΔH is determined from the intercept of the fit with the longitude axis; and $T_{\Delta G0}$ where ΔG equals 0 KJ mol $^{-1}$ is determined from the intercept of the fit with the transversal axis.

It is important to note an increasing slope of the fit of the ΔG versus T relations, i.e. an increasing ΔS , under

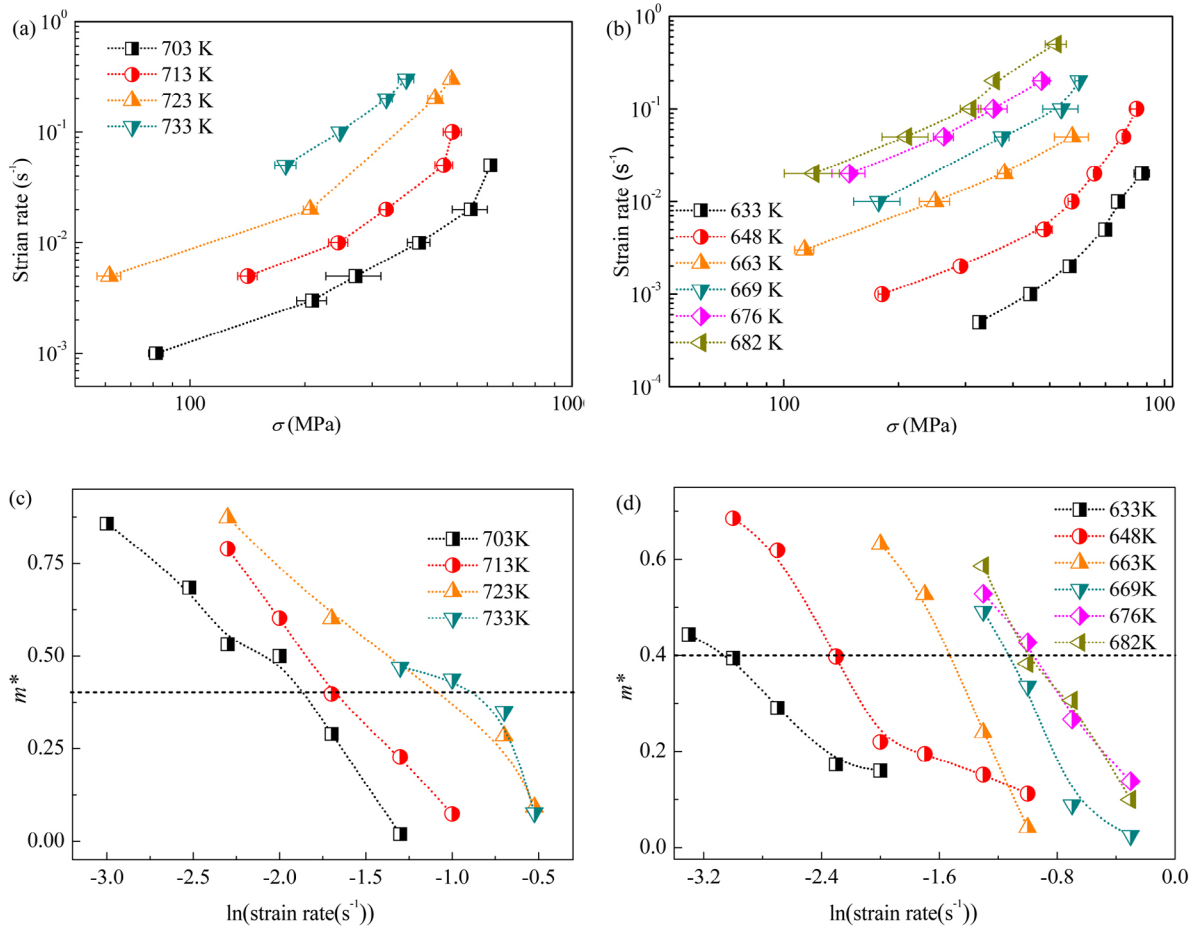


Figure 1. The steady state flow stress of SMLs: (a) Vit106a, (b) Vit1; and the strain rate sensitivity index m^* in the steady flow of SMLs: (c) Vit106a, (d) Vit1. The dotted lines are eye guides.

increasing flow stress for the 2 SMLs. For clarity, figure 3(c) shows the evolution of ΔS under increasing flow stress for Vit106a and Vit1 SMLs. It can be seen that ΔS increases with increasing flow stress, though different increasing tendencies are exhibited. According to the TST, ΔS is the difference of entropy between the initial state and the activated state. Thus, figure 3(c) demonstrates that higher flow stresses lead to more disordered structures, i.e. structural disordering, because larger entropy means more disorder. The structural disordering arises from the phenomenon that the activation of STZs in the flow of SMLs would lead to an increment in the concentration of free volume [29]. A higher free volume concentration indicates a more disordered structure. The observation in figure 3(c) agrees well with the structural disordering observed in the flow of SMLs in previous experimental tests where the increment of free volume concentration is detected [31, 32]. It is also noted that the approximate saturation of ΔS for Vit1 SML at high stress levels is probably due to the extreme of structural ordering is reached, as have been reported in the literatures [31, 32]. Different increasing tendency of ΔS would indicate different rheology dynamics of different SMLs. More details on the picture of the development of structural disordering in the

STZ-mediated flow of SMLs [33, 34] can be found in the seminal work of Argon's [29].

Due to the increasing ΔS under increasing flow stress, the ΔG versus T relations diverge from each other towards higher T , as shown in figures 3(a) and (b). In turn, as illustrated in figure 3(d), a group of $T_{\Delta G0}$ (from 948 K to 1161 K for Vit106a, from 940 to 1078 K for Vit1), rather than a constant value [35], can be observed. It is noted that the liquidus temperature of Vit106a metallic glass is 1110 K [36] and the liquidus temperature of Vit1 metallic glass is 993 K [37], coinciding with the range of $T_{\Delta G0}$. As $T_{\Delta G0}$ represents the temperature where ΔG for flow equals 0 KJ mol⁻¹, it is rational that the 2 groups of $T_{\Delta G0}$ of the 2 SMLs coincide with their liquidus temperature. The group of $T_{\Delta G0}$ can be rationalized with the observation of an underlying polyamorphic transition in the yield of glassy polymers [38] where different flow stresses would incubate different amorphous states which reasonably would lead to different $T_{\Delta G0}$. It is also noted that the compensation effect between ΔS and ΔH in the plastic deformation of metallic glasses has been reported recently [27]. However, an increasing ΔS was not observed, probably due to the different regimes of deformation examined as will be discussed later.

3.2. Glass transition memorized by the enthalpy-entropy compensation

Figures 4(a) and (b) show the linear relationship between ΔH and ΔS of Vit106a and Vit1 SMLs, respectively. It can be seen that the compensation law between ΔH and ΔS is satisfied as $d\Delta H/d\Delta S = T_{MN}$. This linear relationship between ΔH and ΔS is virtually determined by the linear relationship between ΔG and T . The slope of the linear fit of ΔG versus T relation is ΔS . The intercept of the linear fit with the longitude axis is ΔH . Plotted against ΔS , the group of ΔH would exactly collapse onto a line as shown in figures 4(a) and (b), on condition that all the fits of the ΔG versus T relations intersect with each other on the same critical point (see supplemental materials SII). As illustrated in figure 3(d), due to the increasing ΔS under increasing flow stress in shear thinning, the ΔG versus T relations converge towards lower temperature and memorizes a critical temperature $T_{MN} \sim 0.96 T_g$ (657 K and 597 K for Vit106a and Vit1, for which T_g are 683 K and 625 K, respectively), which can be derived from the slope of ΔH versus ΔS relation.

On the ΔG versus T diagram, this critical point indicates that, as T decreases towards T_{MN} , ΔG under different flow stresses increase gradually and become identical as $\sim 178 \text{ KJ mol}^{-1}$ for Vit1 and as $\sim 183 \text{ KJ mol}^{-1}$ for Vit106a (approximately the activation energy of glass transition $\Delta G_g \approx 220 - 250 \text{ KJ mol}^{-1}$ for the 2 SMLs, see supplemental materials SII. Figure S5). Namely, as predicted by the TST, in the steady state flow of SMLs approaching the critical temperature T_{MN} , the strain rates under different flow stresses gradually slow down and approximate a finite small constant value $\dot{\epsilon}_{MN} = \dot{\epsilon}_0 \exp(-\Delta G_{MN}/k_B T_{MN}) \approx 10^{-6} \text{ s}^{-1}$. More importantly, as illustrated in figure 3(d), it is noted that, as the temperature decreases towards T_{MN} , ΔG under a higher flow stress (ΔG_{σ_1} in figure 3(d)) increases faster than ΔG under a lower flow stresses (ΔG_{σ_6} in figure 3(d)), because of the larger activation entropy ΔS under higher flow stresses as shown in figure 3(c). Based on the TST, it means that the flow of SML under higher flow stresses slows down faster, i.e. faster dynamics undergoes faster ‘frozen’, as the temperature decreases towards T_{MN} . More precisely, at the critical point T_{MN} , the flow rate of SML cannot be further increased above 10^{-6} s^{-1} by increasing the flow stress, indicating a diverging resistance to accelerated flow. Namely, as the temperature decreases towards T_{MN} , the enthalpy-entropy compensation requires that the SMLs under different flow stresses should be kinetically ‘frozen’ into an identical solid-like steady flow state [2]. The limit case is that the constant strain rate $\dot{\epsilon}_{MN}$ equals 0 s^{-1} at T_{MN} and the SML becomes a solid, i.e. a glass. It is also noted that a strain rate of 10^{-6} s^{-1} under a steady flow stress of 10^2 MPa corresponds to a viscosity of $10^{14} \text{ Pa} \cdot \text{s}$, which is the typical viscosity value at which the SML is assumed to transit into a glass [2]. Hence this critical point ($T_{MN}, \Delta G_{MN}$) on the ΔG versus T diagram is a clear reminiscent of the thermal glass transition. Considering the ambiguity in the measurement of T_g [39] and the almost consistent activation Gibbs free energy $\Delta G_{MN} \approx \Delta G_g$, the isokinetic temperature $T_{MN} \sim 0.96 T_g$ memorized by the

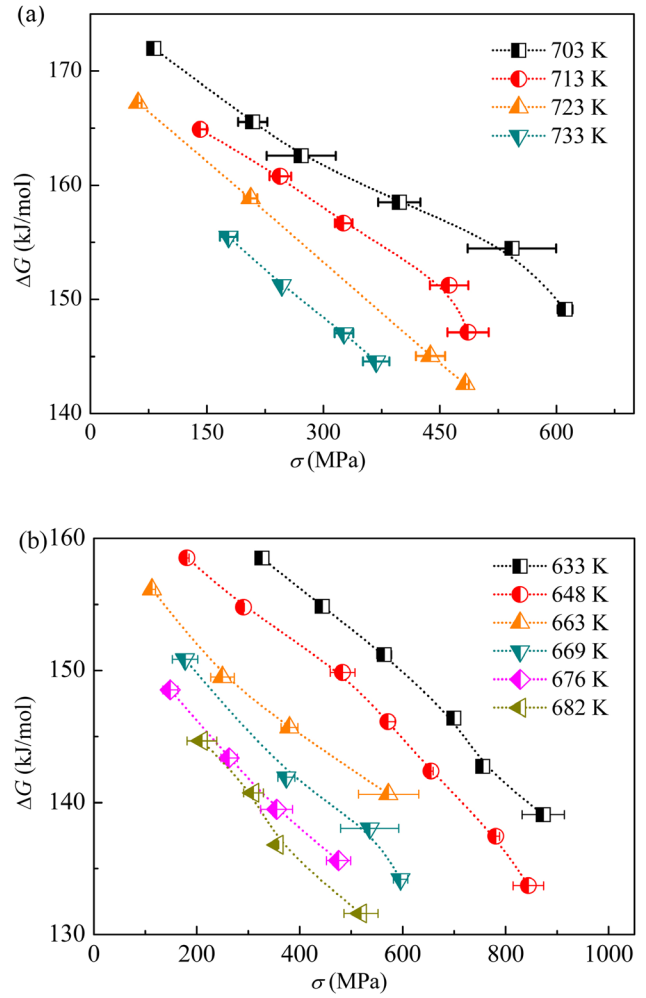


Figure 2. The activation Gibbs free energy versus flow stress (ΔG versus σ) relations in the steady flow of SMLs at different temperatures: (a) Vit106a, (b) Vit1. The dotted lines are eye guides.

$\Delta H - \Delta S$ compensation is concluded to be another version of the glass transition temperature T_g . This memorized glass transition suggests a kinetic nature of the glass forming process. It is of great importance to note that this transition of SMLs into glasses as the temperature approaching T_{MN} (i.e. the SML deviates from its meta-equilibrium state) is virtually memorized by the intrinsic shear disordering of SMLs (i.e. an increasing activation entropy). The memorized glass transition thus suggests an intrinsic correlation between glass forming and shear thinning. The values of T_{MN} at 633 K for Vit1 SML (close to the measured $T_g = 625 \text{ K}$) in figure 3(b) deviating from the linear fit could also be rationalized by the deviation of the Vit1 SML from its meta-equilibrium state as the temperature decrease towards T_{MN} , because closer to the glass transition, the homogeneous steady flow state is getting more difficult to reach in real experimental tests [40]. Moreover, this deviation of ΔG close to T_g also interprets the fact that the current flow data of the 2 SMLs fails to examine the compensation effect in the deformation of metallic glasses in glassy state [27].

More intriguingly, as illustrated in figure 3(d), in the regime where $T < T_{MN}$, a higher flow stress would result

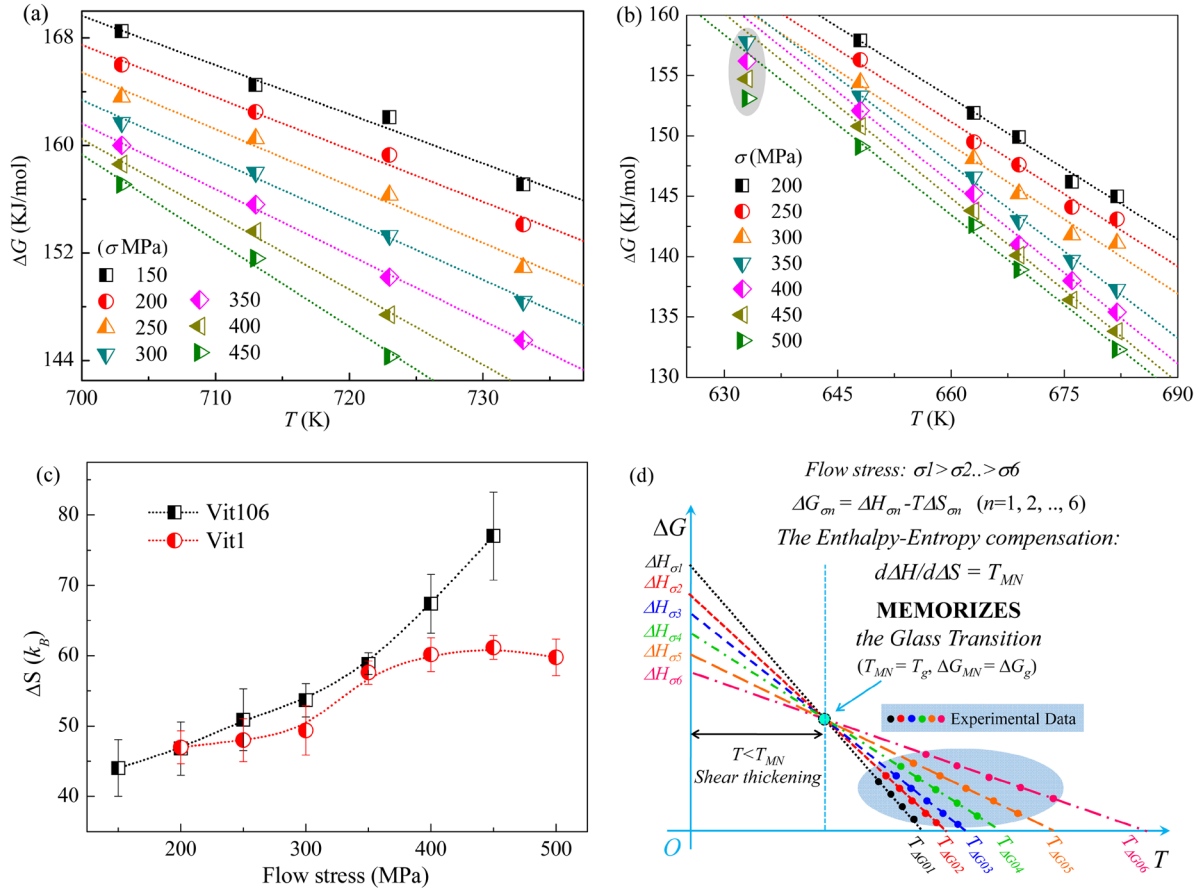


Figure 3. The activation Gibbs free energy versus temperature (ΔG versus T) relations in the shear thinning of Vit106a and Vit1 SMLs: (a) Vit106a, (b) Vit1. The dotted lines are linear fits. The activation entropy ΔS of Vit106a and Vit1 SMLs at different flow stresses (c), indicating the increased disorder in the shear thinning of SMLs. The dotted lines are eye guides. (d) Illustration of the enthalpy-entropy compensation memorized glass transition.

into a higher activation Gibbs free energy ΔG , for instance $\Delta G_{\sigma 1} > \Delta G_{\sigma 6}$. In the TST, a higher activation Gibbs free energy ΔG means a lower flow rate and in turn indicates a higher viscosity. This phenomenon is the well known ‘shear thickening’, where higher flow rate causes higher viscosity. Thus, the enthalpy-entropy compensation law predicts a shear thickening regime in the flow of SMLs on the ΔG versus T diagram where $T < T_{MN}$. This shear thickening regime at $T < T_{MN}$ also supports the above conclusion that the critical point ($T_{MN}, \Delta G_{MN}$) on the ΔG versus T diagram is a virtually a kinetic glass transition. To our best knowledge, the shear thickening regime has not been observed in metallic glasses [40]. The reason for the not observed shear thickening regime in metallic glasses is probably due to the fact the homogeneous steady state flow of SMLs in the $T < T_{MN}$ regime (i.e. in glassy state) cannot be reached in real experimental tests, where the highly inhomogeneous shear bands-mediated plastic deformation of metallic glasses [40] dominates the flow. However, the shear thickening phenomenon has already been observed in quite a few glass-like systems [41, 42]. In future, the potential existence of a shear thickening regime in the flow of SMLs is of fundamental significance and worthy of more intensive investigations.

3.3. Origin of the enthalpy-entropy compensation in SMLs

Inspired by the microscopic explanation of the enthalpy-entropy compensation provided by Yelon and Movaghar [17], the origin of the enthalpy-entropy compensation law in the shear thinning of SMLs can be revealed as follows. As proposed by Boisvert *et al* [18], the enthalpy-entropy compensation effect in the thermally assisted activation process exhibits a many-body nature, which means that the activation energy for the activation process is provided by multiple typical elementary excitations. To provide the activation energy for the activation process, the multiple excitations are assembled in a collective mode [17]. In the SMLs, the activation process is the flow of SMLs and the typical excitation is the STZ event. In the flow of SMLs, the STZs are assembled in a collective mode [43]. With an increased number of the collectively activated STZs, the number of ways of assembling these STZs (i.e. the routes to the activated state) increases exponentially. It is the growth in the activation routes that results into an increased activation entropy ΔS under increasing flow stresses which comprises the entropic compensation effect [18].

This proposition has been verified in a model glass where the entropy of combining multiple STZs to overcome the

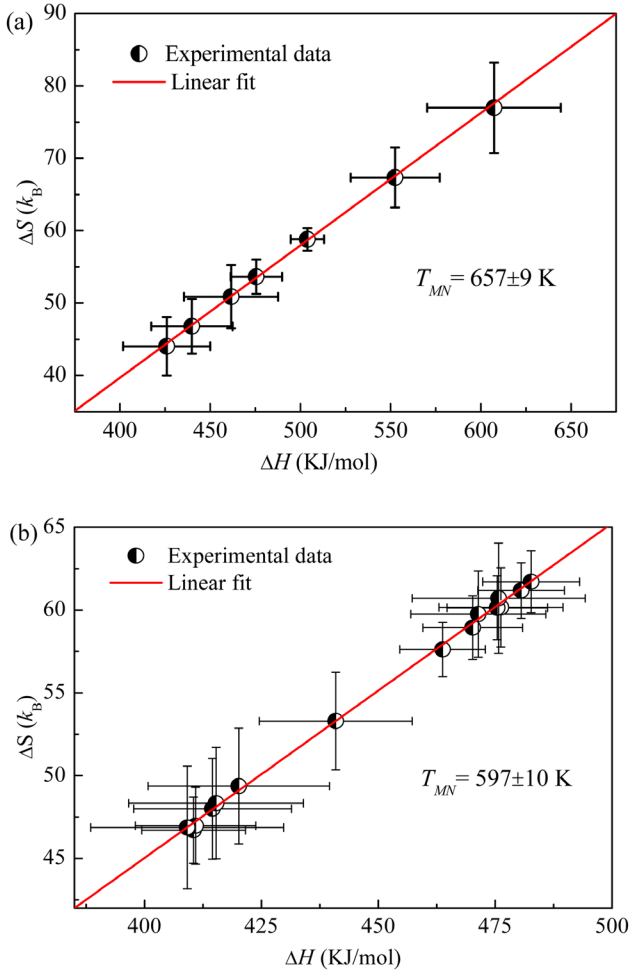


Figure 4. The linear relationship between activation enthalpy ΔH and activation entropy ΔS in the shear thinning of Vit106a (a) and Vit1 (b) SMLs. The solid lines are linear fits.

energy barrier for flow constituents the enthalpy-entropy compensation effect [22]. To further confirm this proposition in our work, it is noted that the increased number of collectively activated STZs corresponds to the increment of the activation volume V [17]. The STZs activated in a multiple-STZs collective mode will feel a larger activation volume. Similar collective mode indicated by the increased activation volume is also observed in the nucleation of dislocations [44]. Therefore, the increased ΔS in the enthalpy-entropy compensation law under increasing flow stress suggests a concomitantly increased activation volume V . The activation volume $V = -\partial\Delta G(\sigma, T)/\partial\sigma$ for the flow of the 2 SMLs can be derived via introducing $\Delta G(T, \sigma) = k_B T \ln(\dot{\epsilon}_0/\dot{\epsilon})$. As having been established [45], the activation volume V reads: $V \propto \frac{k_B T}{\sigma m^*}$, where $m^* = \partial \ln \sigma / \partial \ln \dot{\epsilon}$ is the strain rate sensitivity index.

For convenience, figure 5 shows the value of $\sigma \cdot m^*$ instead of the $k_B T / \sigma m^*$ of Vit106a and Vit1 SMLs in steady state flow, respectively, where the main results remain unchanged. It can be seen that for both of the 2 SMLs, $\sigma \cdot m^*$ increases, i.e. V decreases, in an initial shear thinning regime ($m^* > 0.4$, as indicated by the dashed line in figures 1(c) and (d)). While in a prominent shear thinning regime $m^* < 0.4$, $\sigma \cdot m^*$

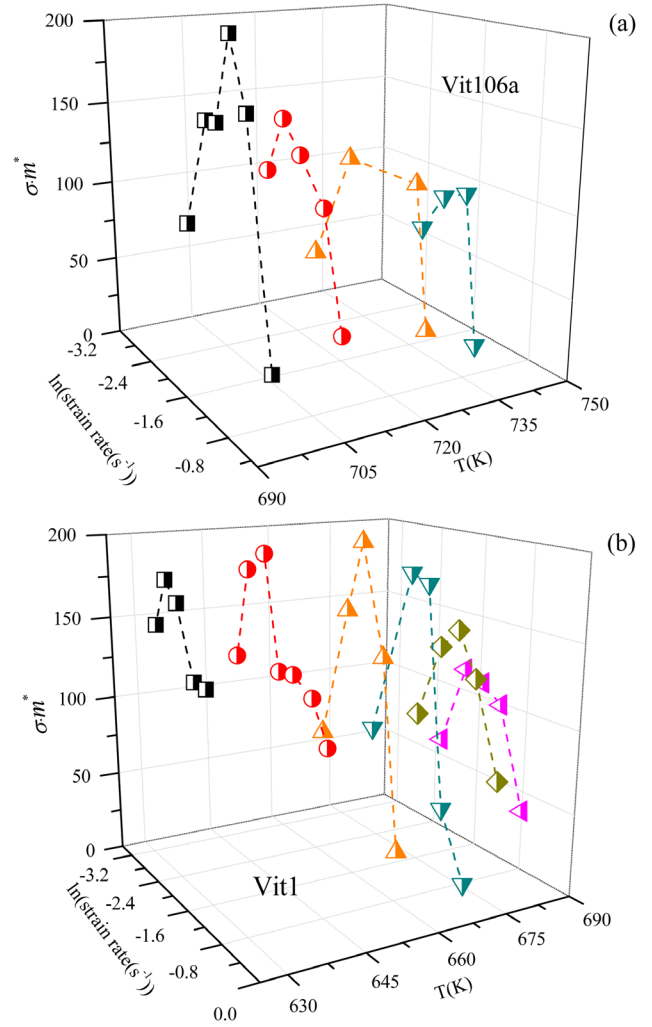


Figure 5. The product of flow stress and strain rate sensitivity index: $\sigma \cdot m^*$ at different temperatures of SMLs: (a) Vit106a and (b) Vit1. The dashed lines are eye guides.

decreases, i.e. V increases. The 2 shear thinning regimes have also been observed in the creep of metallic glasses [46], which correspond to 2 different deformation mechanisms, i.e. single atom diffusion (or sparse STZs, $n = 1/m^* < 2.5$) and cluster cooperative shear transformation (or multiple STZs, $n = 1/m^* > 2.5$), respectively. This phenomenon also coincides with the fact that $m^* \approx 0.4 - 0.6$ has been reported as the boundary for the development of long range correlation in the steady flow state of sheared glasses and emulsions [12, 47]. Thus, the decrease of $\sigma \cdot m^*$, i.e. increase of V , in the prominent shear thinning regime $m^* < 0.4$ indicates the development of strong correlation effects between STZs [48], which would lead to the collective activation of STZs. The larger V in the collective activation of STZs, the more routes to the activated state. Hence, the increment of V is concluded to be the main cause for the increment of ΔS at higher flow stresses in the prominent shear thinning regime $m^* < 0.4$ of SMLs, i.e. the origin of the enthalpy-entropy compensation. Additionally, it is intriguing to see the initial shear thinning regime $m^* > 0.4$, where $\sigma \cdot m^*$ increases, i.e. V decreases. In this regime, as predicted in simulations and emulsions [12, 47], the correlation effect is not dominant. The enthalpy-entropy

compensation effect, i.e. the increment of ΔS at increasing flow stresses, is probably due to the increased number of the sparsely distributed STZs arising from the facilitation effect in the activation STZs. The result in figure 5 is in alignment with the competition between the facilitation and correlation effects in the flow of SMLs [48]. These findings enrich current understanding on the many-body nature of the ubiquitous enthalpy-entropy compensation law.

Moreover, to further understand the origin of the enthalpy-entropy compensation in SMLs, it is important to note that the compensation effect has also been found to apply to the grain boundary internal friction [49] and dislocation nucleation from the inside of grain boundaries [44]. The atomic structure inside grain boundaries bears a strong resemblance to the amorphous structure of metallic glasses. More importantly, the enthalpy-entropy compensation temperature of the grain boundary internal friction in high purity aluminum also locates at a critical phase transition point [49], below which the relaxation process in grain boundary internal friction with a lower activation enthalpy is faster, while above which the relaxation process with a higher activation enthalpy is faster. This crossover of the relaxation time of the relaxation process in grain boundary internal friction at the compensation temperature is much similar to the memorized glass transition in the current work, below which the flow of SMLs with a lower activation enthalpy is faster, while above which the flow of SMLs with a higher activation enthalpy is faster. The synchronization (i.e. a collective mode) of the relaxation units in the grain boundary internal friction is also considered crucial in the crossover of the relaxation time [49]. On the other hand, the nucleation mechanism of dislocations from the inside of grain boundaries also exhibits a transition from a shuffling-assisted mode to a collective nucleation mode upon increasing flow rate [44]. This fact highly coincides with the transition from sparsely activated STZs to the collectively activated STZs in the flow mechanism of SMLs. Especially, similar variation tendency of the activation volume shown in figure 5 is also found for the dislocation nucleation from the inside of grain boundaries. More works on these issues in future would largely advance our knowledge on the universality of the enthalpy-entropy compensation law.

4. Conclusion

In summary, the enthalpy-entropy compensation law are examined in the shear thinning regime of 2 typical SMLs. A group of ΔG versus T relations diverging from each other towards higher temperature, i.e. converging towards lower temperature, are observed in the shear thinning of SMLs. The ΔG versus T relations indicate an increasing activation entropy ΔS , i.e. increasing disorder, under increasing flow stress and suggest a polyamorphic transition in the yield of metallic glasses. The enthalpy-entropy compensation memorizes the glass transition in the strongly shear-thinned SMLs, demonstrating a kinetic nature of glass transition. The enthalpy-entropy compensation effect is attributed to the facilitation effect and the correlation effect in the activation of STZs, in

the initial shear thinning regime and in the prominent shear thinning regime divided by a critical strain rate sensitivity index $m^* \approx 0.4$, respectively.

Acknowledgments

This work was financially supported by the National Nature and Science Foundation of China under grant No. 51701082 and by ‘the Fundamental Research Funds for the Central Universities’.

ORCID iDs

Meng Zhang  <https://orcid.org/0000-0002-2439-5452>

References

- [1] Berthier L and Biroli G 2011 Theoretical perspective on the glass transition and amorphous materials *Rev. Mod. Phys.* **83** 587–645
- [2] Debenedetti P G and Stillinger F H 2001 Supercooled liquids and the glass transition *Nature* **410** 259–67
- [3] Angell C A, Ngai K L, McKenna G B, McMillan P F and Martin S W 2000 Relaxation in glassforming liquids and amorphous solids *J. Appl. Phys.* **88** 3113–57
- [4] Yamamoto R and Onuki A 2000 Dynamics of highly supercooled liquids far from equilibrium *J. Phys.: Condens. Matter* **12** 6323–34
- [5] Berthier L and Barrat J-L 2002 Shearing a glassy material: numerical tests of nonequilibrium mode-coupling approaches and experimental proposals *Phys. Rev. Lett.* **89** 095702
- [6] Fuchs M and Cates M E 2002 Theory of nonlinear rheology and yielding of dense colloidal suspensions *Phys. Rev. Lett.* **89** 248304
- [7] O’Hern C S, Liu A J and Nagel S R 2004 Effective temperatures in driven systems: static versus time-dependent relations *Phys. Rev. Lett.* **93** 165702
- [8] Katgert G, Mobius M E and van Hecke M 2008 Rate dependence and role of disorder in linearly sheared two-dimensional foams *Phys. Rev. Lett.* **101** 058301
- [9] Furukawa A, Kim K, Saito S and Tanaka H 2009 Anisotropic cooperative structural rearrangements in sheared supercooled liquids *Phys. Rev. Lett.* **102** 016001
- [10] Langer J S 2014 Theories of glass formation and the glass transition *Rep. Prog. Phys.* **77** 042501
- [11] Viasnoff V and Lequeux F 2002 Rejuvenation and overaging in a colloidal glass under shear *Phys. Rev. Lett.* **89** 065701
- [12] Haxton T K and Liu A J 2007 Activated dynamics and effective temperature in a steady state sheared glass *Phys. Rev. Lett.* **99** 195701
- [13] Yu H B, Richert R, Maass R and Samwer K 2015 Unified criterion for temperature-induced and strain-driven glass transitions in metallic glass *Phys. Rev. Lett.* **115** 135701
- [14] Guan P F, Chen M W and Egami T 2010 Stress-temperature scaling for steady-state flow in metallic glasses *Phys. Rev. Lett.* **104** 205701
- [15] Liu Y H, Liu C T, Wang W H, Inoue A, Sakurai T and Chen M W 2009 Thermodynamic origins of shear band formation and the universal scaling law of metallic glass strength *Phys. Rev. Lett.* **103** 065504
- [16] Zhang M, Wang Y M, Li F X, Jiang S Q, Li M Z and Liu L 2017 Mechanical relaxation-to-rejuvenation transition in a Zr-based bulk metallic glass *Sci. Rep.* **7** 625

- [17] Yelon A and Movaghar B 1990 Microscopic explanation of the compensation (Meyer–Neldel) rule *Phys. Rev. Lett.* **65** 618–20
- [18] Boisvert G, Lewis L J and Yelon A 1995 Many-body nature of the Meyer–Neldel compensation law for diffusion *Phys. Rev. Lett.* **75** 469–72
- [19] Ryu S, Kang K and Cai W 2011 Entropic effect on the rate of dislocation nucleation *Proc. Natl Acad. Sci. USA* **108** 5174–8
- [20] Gehrig J C, Penedo M, Parschau M, Schwenk J, Marioni M A, Hudson E W and Hug H J 2017 Surface single-molecule dynamics controlled by entropy at low temperatures *Nat. Commun.* **8** 14404
- [21] Yelon A, Movaghar B and Crandall R S 2006 Multi-excitation entropy: its role in thermodynamics and kinetics *Rep. Prog. Phys.* **69** 1145–94
- [22] Koziatek P, Barrat J-L, Derlet P and Rodney D 2013 Inverse Meyer–Neldel behavior for activated processes in model glasses *Phys. Rev. B* **87** 224105
- [23] Falk M L and Langer J S 2011 Deformation and failure of amorphous, solidlike materials *Annual Rev. Condens. Matter Phys.* **2** 353–73
- [24] Langer J S 2004 Dynamics of shear-transformation zones in amorphous plasticity: formulation in terms of an effective disorder temperature *Phys. Rev. E* **70** 041502
- [25] Hedges L O, Jack R L, Garrahan J P and Chandler D 2009 Dynamic order-disorder in atomistic models of structural glass formers *Science* **323** 1309–13
- [26] Cheng Y Q and Ma E 2011 Atomic-level structure and structure–property relationship in metallic glasses *Prog. Mater. Sci.* **56** 379–473
- [27] Wang Y J, Zhang M, Liu L, Ogata S and Dai L H 2015 Universal enthalpy-entropy compensation rule for the deformation of metallic glasses *Phys. Rev. B* **92** 174118
- [28] Argon A S and Kuo H Y 1979 Plastic flow in a disordered bubble raft (an analog of a metallic glass) *Mater. Sci. Eng.* **39** 101–9
- [29] Argon A S 1979 Plastic deformation in metallic glasses *Acta Metall.* **27** 47–58
- [30] Berthier L and Barrat J L 2002 Nonequilibrium dynamics and fluctuation-dissipation relation in a sheared fluid *J. Chem. Phys.* **116** 6228–42
- [31] de Hey P, Sietsma J and van den Beukel A 1998 Structural disordering in amorphous Pd₄₀Ni₄₀P₂₀ induced by high temperature deformation *Acta Mater.* **46** 5873–82
- [32] Tong Y, Iwashita T, Dmowski W, Bei H, Yokoyama Y and Egami T 2015 Structural rejuvenation in bulk metallic glasses *Acta Mater.* **86** 240–6
- [33] Lacks D J 2001 Energy landscapes and the non-Newtonian viscosity of liquids and glasses *Phys. Rev. Lett.* **87** 225502
- [34] Lubchenko V 2009 Shear thinning in deeply supercooled melts *Proc. Natl Acad. Sci. USA* **106** 11506–10
- [35] Boots H M J and De Bokx P K 1989 Theory of enthalpy-entropy compensation *J. Phys. Chem.* **93** 8240–3
- [36] Gallino I, Shah M B and Busch R 2007 Enthalpy relaxation and its relation to the thermodynamics and crystallization of the Zr_{58.5}Cu_{15.6}Ni_{12.8}Al_{10.3}Nb_{2.8} bulk metallic glass-forming alloy *Acta Mater.* **55** 1367–76
- [37] Busch R, Kim Y J and Johnson W L 1995 Thermodynamics and kinetics of the undercooled liquid and the glass transition of the Zr_{41.2}Ti_{13.8}Cu_{12.5}Ni_{10.0}Be_{22.5} alloy *J. Appl. Phys.* **77** 4039–43
- [38] McKenna G B 2003 Mechanical rejuvenation in polymer glasses: fact or fallacy? *J. Phys.: Condens. Matter* **15** S737–63
- [39] Evenson Z, Gallino I and Busch R 2010 The effect of cooling rates on the apparent fragility of Zr-based bulk metallic glasses *J. Appl. Phys.* **107** 123529
- [40] Schuh C A, Hufnagel T and Ramamurty U 2007 Mechanical behavior of amorphous alloys *Acta Mater.* **55** 4067–109
- [41] Cheng X, McCoy J H, Israelachvili J N and Cohen I 2011 Imaging the microscopic structure of shear thinning and thickening colloidal suspensions *Science* **333** 1276–9
- [42] Fall A, Lemaitre A, Bertrand F, Bonn D and Ovarlez G 2010 Shear thickening and migration in granular suspensions *Phys. Rev. Lett.* **105** 268303
- [43] Homer E R, Rodney D and Schuh C A 2010 Kinetic Monte Carlo study of activated states and correlated shear-transformation-zone activity during the deformation of an amorphous metal *Phys. Rev. B* **81** 064204
- [44] Du J-P, Wang Y-J, Lo Y-C, Wan L and Ogata S 2016 Mechanism transition and strong temperature dependence of dislocation nucleation from grain boundaries: an accelerated molecular dynamics study *Phys. Rev. B* **94** 104110
- [45] Asaro R J and Suresh S 2005 Mechanistic models for the activation volume and rate sensitivity in metals with nanocrystalline grains and nano-scale twins *Acta Mater.* **53** 3369–82
- [46] Cao P, Short M P and Yip S 2017 Understanding the mechanisms of amorphous creep through molecular simulation *Proc. Natl Acad. Sci.* **114** 13631–6
- [47] Mason T G, Bibette J and Weitz D A 1996 Yielding and flow of monodisperse emulsions *J. Colloid Interface Sci.* **179** 439–48
- [48] Zhang M, Liu L and Wu Y 2013 Facilitation and correlation of flow in metallic supercooled liquid *J. Chem. Phys.* **139** 164508
- [49] Jiang W B, Kong Q P, Molodov D A and Gottstein G 2009 Compensation effect in grain boundary internal friction *Acta Mater.* **57** 3327–31